FÍSICA
MATEMÁTICAS
COMPUTACIÓN

Curro PB

CEAFMC-UHU

Notes on Coupled Kerr Resonators

1. Quantum Hamiltonian

Following [1, 2] and using our notation for the parameters, the quantum effective Hamiltonian for N coupled Kerr transmons with two-photon squeezing is

$$\hat{H} = \sum_{i=1}^{N} \hat{H}_i + \hat{H}_c = \sum_{i=1}^{N} \left[-\Delta_i \hat{n}_i + K_i \hat{a}_i^{\dagger 2} \hat{a}_i^{\,2} - \epsilon_{2,i} \left(\hat{a}_i^{\dagger 2} + \hat{a}_i^{\,2} \right) \right] - \epsilon_c \sum_{i=1}^{N} \sum_{j=1}^{N} J_{ij} \hat{a}_i^{\dagger} \hat{a}_j \ , \quad (1.1)$$

where $J_{ij} = J_{ji}$ and $J_{ii} = 0$.

Note that it can be checked that the interactions in the Hamiltonian connect states in the coupled Fock space such that one can split the Hilbert space into two blocks, depending on the parity of $n_1 + n_2$.

If the N coupled Kerr transmons can be considered identical, $\Delta_i = \Delta$, $K_i = K$, and $\epsilon_{2,i} = \epsilon_2$ and we can scale the Hamiltonian (1.1) by the Kerr parameter K

$$\hat{\mathcal{H}} = \frac{\hat{H}}{K} = \sum_{i=1}^{N} \left[-\delta \hat{n}_i + \hat{a}_i^{\dagger 2} \hat{a}_i^{\,2} - \xi_2 \left(\hat{a}_i^{\dagger 2} + \hat{a}_i^{\,2} \right) \right] - \xi_c \sum_{i=1}^{N} \sum_{j=1}^{N} J_{ij} \hat{a}_i^{\dagger} \hat{a}_j \ , \quad (1.2)$$

where $\delta = \Delta/K$, $\xi_2 = \epsilon_2/K$, and $\xi_c = \epsilon_c/K$ are scaled parameters.

In the case of identical KPOs then the Hilbert space can be further split according to the irreps of the symmetric group $\mathcal{S}_N$, where N is the number of coupled KPOs.

If we assume that we have only two coupled oscillators, $N_c = 2$, and the quantum Hamiltonian $\hat{\mathcal{H}} = \frac{\hat{H}}{K}$ is

$$\begin{aligned} \hat{\mathcal{H}} = & -\delta(\hat{n}_1 + \hat{n}_2) + \hat{a}_1^{\dagger 2} \hat{a}_1^{\,2} + \hat{a}_2^{\dagger 2} \hat{a}_2^{\,2} - \xi_2 \left(\hat{a}_1^{\dagger 2} + \hat{a}_1^{\,2} + \hat{a}_2^{\dagger 2} + \hat{a}_2^{\,2} \right) \\ & - \xi_c J_{12} \left(\hat{a}_1^{\dagger} \hat{a}_2 + \hat{a}_2^{\dagger} \hat{a}_1 \right) \ . \end{aligned} \quad (1.3)$$

In this case the Hilbert space can be split into four blocks, depending on the parity of the total number of quanta and the symmetric or antisymmetric character under $\mathcal{S}_2$ permutation. If the two Kerr resonators are not identical then $\hat{\mathcal{H}}' = \frac{\hat{H}}{K_1}$ is

$$\begin{aligned} \hat{\mathcal{H}}' = & -\delta_1 \hat{n}_1 - \delta_2 \hat{n}_2 + \hat{a}_1^{\dagger 2} \hat{a}_1^{\,2} + \kappa \hat{a}_2^{\dagger 2} \hat{a}_2^{\,2} - \xi_{2,1} \left(\hat{a}_1^{\dagger 2} + \hat{a}_1^{\,2} \right) - \xi_{2,2} \left(\hat{a}_2^{\dagger 2} + \hat{a}_2^{\,2} \right) \\ & - \xi_c J_{12} \left(\hat{a}_1^{\dagger} \hat{a}_2 + \hat{a}_2^{\dagger} \hat{a}_1 \right) \ , \end{aligned} \quad (1.4)$$

where all parameters have been scaled by K_1 and $\kappa = K_2/K_1$. Hamiltonian matrix elements for the non-identical Kerr oscillator case are

$$\begin{aligned} \left\langle n_1, n_2 | \hat{\mathcal{H}}' | n_1, n_2 \right| n_1, n_2 | \hat{\mathcal{H}}' | n_1, n_2 \Big\rangle &= -\delta_1 n_1 - \delta_2 n_2 + n_1(n_1 - 1) + \kappa n_2(n_2 - 1) \\ \left\langle n_1 + 2, n_2 | \hat{\mathcal{H}}' | n_1, n_2 \right| n_1 + 2, n_2 | \hat{\mathcal{H}}' | n_1, n_2 \Big\rangle &= -\xi_{2,1} \sqrt{(n_1 + 1)(n_1 + 2)} \\ \left\langle n_1, n_2 + 2 | \hat{\mathcal{H}}' | n_1, n_2 \right| n_1, n_2 + 2 | \hat{\mathcal{H}}' | n_1, n_2 \Big\rangle &= -\xi_{2,2} \sqrt{(n_2 + 1)(n_2 + 2)} \\ \left\langle n_1 + 1, n_2 - 1 | \hat{\mathcal{H}}' | n_1, n_2 \right| n_1 + 1, n_2 - 1 | \hat{\mathcal{H}}' | n_1, n_2 \Big\rangle &= -\xi_c J_{12} \sqrt{(n_1 + 1) n_2} \ , \end{aligned} \quad (1.5)$$

where it is clear that states with even(odd) n_1+n_2 values only can be connected to states with even(odd) total number of quanta.

If we truncate the Fock basis for the i-th resonator at dim_i, the Hamiltonian for each of the single Kerr oscillators has a C_2 symmetry, and the Hamiltonian matrix can be split into even and odd symmetry blocks. However, this symmetry is broken by the inclusion coupling term, that transfers one quanta of excitation between the two resonators. Therefore the dimension of the Hilbert space for the two coupled resonators is $dim_1 \times dim_2$. In the case of identical resonators, as in Hamiltonian (1.3), the Hamiltonian matrix can be split into sub-blocks that are symmetric or antisymmetric under the interchange of the particles.

We will characterize the eigenstates using two quantitites, the participation ratio, PR, and the entanglement entropy, S_1.

Entanglement entropy The entanglement entropy, S_1, calculation requires first the tracing of the density matrix of the system's eigenvectors with respect to one of the two subsystems. As this is a bipartite entanglement entropy, it is independent on what subsystem are you tracing out. In particular, we trace over subsystem 2 and obtain the partial density matrix $\rho_1 = Tr_2(\rho)$ for each eigenvector. Then, the partial density matrix is diagonalized (to transform into a Schmidt decomposition) and the entanglement entropy is computed as

$$S_1 = -\sum_k \lambda_k \log(\lambda_k) \ , \tag{1.6}$$

where λ_k are the partial density matrix ρ_1 eigenvalues. The entanglement entropy is zero for product states (all the eigenvalues are zero besides one of them that is unity) and its value increases for entangled states.

Participation ratio The participation ratio, PR, has the usual definition, for a state expressed in the Fock basis as $|\Psi\rangle = \sum_k C_k |n\rangle$,

$$PR_\Psi = \frac{1}{\sum_k |C_k|^4} \ . \tag{1.7}$$

2. Classical limit analysis

We can obtain the classical limit of the coupled Kerr Hamiltonians (1.3) and (1.4) from [1] or computing the classical limit using the definition of creation and annihilation harmonic operators as functions of unitless coordinate $\hat{q}_k$ and momentum $\hat{p}_k$ for the k-th oscillator [3]

$$a_k^\dagger = \sqrt{\frac{N_e}{2}}(\hat{q}_k - i\hat{p}_k) \ , \quad a_k = \sqrt{\frac{N_e}{2}}(\hat{q}_k + i\hat{p}_k) \quad k = 1, 2 \ . \tag{2.1}$$

Using this definition $[\hat{q}_j, \hat{p}_k] = \delta_{j,k}\frac{i}{N_e}$, $[a_k, a_k^\dagger] = 1$ and, in the classical limit, $[q_k, p_k] = 0$. Taking into account that

$$\hat{n}_k = a_k^\dagger a_k = \frac{N_e}{2}\left(\hat{p}_k^2 + \hat{q}_k^2 - \frac{1}{N_e}\right) ,$$
$$a_k^{\dagger\,2} + a_k^2 = N_e\left(\hat{q}_k^2 - \hat{p}_k^2\right) ,$$
$$a_k^{\dagger\,2} a_k^2 = \hat{n}_k(\hat{n}_k - 1) = \frac{N_e^2}{4}\left(\hat{p}_k^4 + \hat{q}_k^4 + \hat{p}_k^2\hat{q}_k^2 + \hat{q}_k^2\hat{p}_k^2\right) - N_e\left(\hat{p}_k^2 + \hat{q}_k^2\right) + \frac{3}{4} ,$$
$$a_k^\dagger a_j + a_j^\dagger a_k = N_e\left(\hat{p}_k\hat{p}_j + \hat{q}_k\hat{q}_j\right) ,$$

with $k = 1, 2$. Substituting in Eqs. (1.3) and (1.4) we obtain a classical Hamiltonian that can be expressed as a function of the $\hat{q}_k$ and $\hat{p}_k$ conjugate operators. One has to multiply one-body terms times N_e. In the identical KPOs case (1.3), the classical ($N_e \to \infty$ limit) Hamiltonian is

$$\mathcal{H} = \frac{H}{\hbar K N_e^2} = -\frac{\delta}{2}\sum_{k=1}^{N_c=2}\left(p_k^2 + q_k^2\right) + \frac{1}{4}\sum_{k=1}^{N_c=2}\left(p_k^2 + q_k^2\right)^2 - \xi_2\sum_{k=1}^{N_c=2}\left(q_k^2 - p_k^2\right) - \xi_c J_{12}\left(p_1p_2 + q_1q_2\right) . \tag{2.2}$$

In the non-identical resonators case (1.4), the classical limit of the quantum Hamiltonian is

$$\mathcal{H} = -\delta_1\left(p_1^2 + q_1^2\right) - \delta_2\left(p_2^2 + q_2^2\right) + \frac{1}{4}\left(p_1^2 + q_1^2\right)^2 + \frac{\kappa}{4}\left(p_2^2 + q_2^2\right)^2 \tag{2.3}$$
$$- \xi_{2,1}\left(q_1^2 - p_1^2\right) - \xi_{2,2}\left(q_2^2 - p_2^2\right) - \xi_c J_{12}\left(p_1p_2 + q_1q_2\right) . \tag{2.4}$$

textcolorblueLet's consider the following change of variables:

$$\begin{cases} q_i^2 + p_i^2 &= a_i \\ q_i^2 - p_i^2 &= b_i \end{cases} \Longrightarrow \begin{cases} q_i &= \sqrt{\frac{a_i + b_i}{2}} \\ p_i &= \sqrt{\frac{a_i - b_i}{2}} \end{cases} \tag{2.5}$$

in Hamiltonian (2.4)

$$\mathcal{H} = -\delta_1 a_1 - \delta_2 a_2 + \frac{1}{4}a_1^2 + \frac{\kappa}{4}a_2^2 - \xi_{2,1}b_1 - \xi_{2,2}b_2 - \xi_c J_{12}\sqrt{\frac{a_1a_2 + b_1b_2}{2}} . \tag{2.6}$$

3. Phase Diagram for two KPOs

Starting point

$$\mathcal{H}(\mathbf{q},\mathbf{p}) = -\frac{\delta}{2}\left(p_1^2 + p_2^2 + q_1^2 + q_2^2\right) + \frac{1}{4}\left(p_1^2 + q_1^2\right)^2 + \frac{1}{4}\left(p_2^2 + q_2^2\right)^2$$
$$- \xi_2\left(q_1^2 + q_2^2 - p_1^2 - p_2^2\right) - \xi_c J_{12}\left(p_1p_2 + q_1q_2\right) . \tag{3.1}$$

To approach this problem, we will consider the following change of variables:

$$\begin{cases} p_i &= r_i\sin(\theta_i) \\ q_i &= r_i\cos(\theta_i) \end{cases} , \tag{3.2}$$

being the hessian determinant $\|\frac{\partial x_i}{\partial q_j}\| = r_1r_2$. The Hamiltonian (3.1) turns into

$$-\frac{\delta}{2}\left(r_1^2 + r_2^2\right) + \frac{1}{4}\left(r_1^4 + r_2^4\right) - \xi\left[r_1^2\cos(2\theta_1) + r_2^2\cos(2\theta_2)\right] - Jr_1r_2\cos(\theta_1 - \theta_2) , \tag{3.3}$$

where we have redefined the control parameters as $\xi = \xi_2$ and $J = \xi_c J_{12}$.

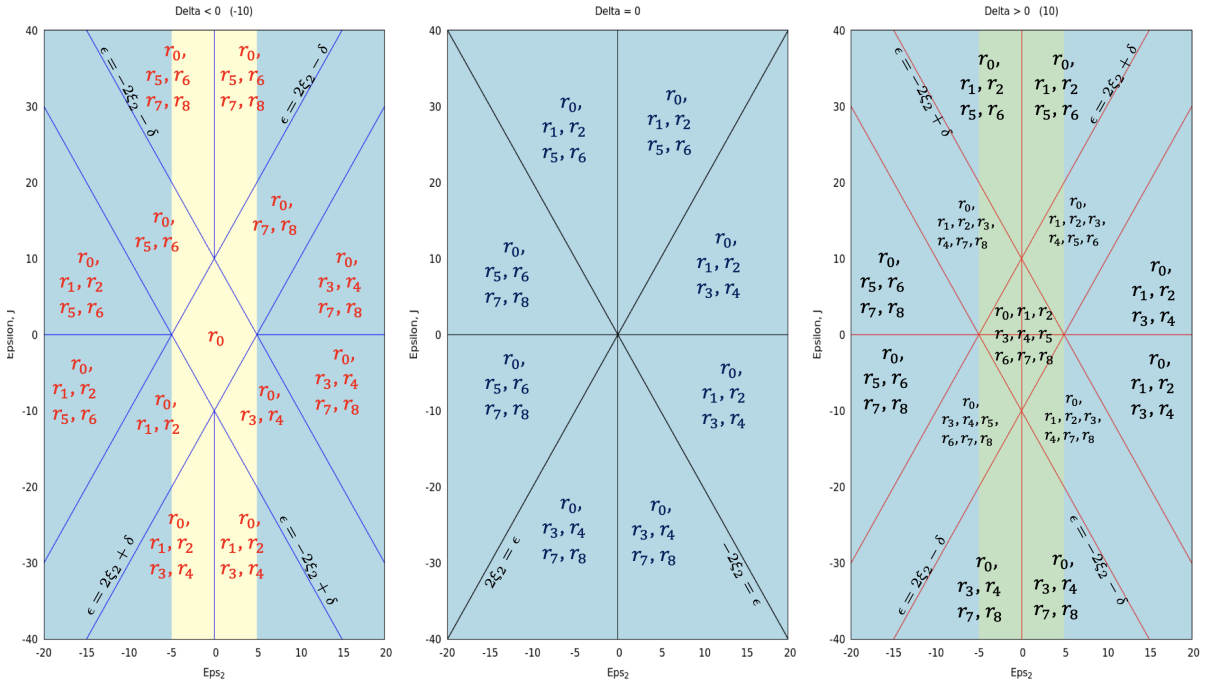

Figure 3.1: Phase space transitions in the parameter diagram. On the left, the diagram corresponds to a negative value of δ. In blue, it shows the case where the two uncoupled Kerr oscillators have a phase space with two minima and a hyperbolic point; in yellow, the case of two coupled Kerr oscillators with a phase space featuring only one minimum. In the center, the diagram for $\delta = 0$ is displayed. In this case, regardless of the parameter, the uncoupled Kerr oscillators exhibit a phase space with two minima and a hyperbolic point. On the right, for $\delta > 0$, shown in green, the uncoupled Kerr oscillators present a phase space with two minima, two hyperbolic points, and a maximum.

3.1 Stationary points

$r_j =$	q_1	q_2	p_1	p_2	Energy
$r_0 =$	0	0	0	0	0
$r_1 =$	$\sqrt{\delta + 2\xi_2 + \epsilon}$	$\sqrt{\delta + 2\xi_2 + \epsilon}$	0	0	$-(\delta + 2\xi_2 + \epsilon)^2/2$
$r_2 =$	$-\sqrt{\delta + 2\xi_2 + \epsilon}$	$-\sqrt{\delta + 2\xi_2 + \epsilon}$	0	0	$-(\delta + 2\xi_2 + \epsilon)^2/2$
$r_3 =$	$\sqrt{\delta + 2\xi_2 - \epsilon}$	$-\sqrt{\delta + 2\xi_2 - \epsilon}$	0	0	$-(\delta + 2\xi_2 - \epsilon)^2/2$
$r_4 =$	$-\sqrt{\delta + 2\xi_2 - \epsilon}$	$\sqrt{\delta + 2\xi_2 - \epsilon}$	0	0	$-(\delta + 2\xi_2 - \epsilon)^2/2$
$r_5 =$	0	0	$\sqrt{\delta - 2\xi_2 + \epsilon}$	$\sqrt{\delta - 2\xi_2 + \epsilon}$	$-(\delta - 2\xi_2 + \epsilon)^2/2$
$r_6 =$	0	0	$-\sqrt{\delta - 2\xi_2 + \epsilon}$	$-\sqrt{\delta - 2\xi_2 + \epsilon}$	$-(\delta - 2\xi_2 + \epsilon)^2/2$
$r_7 =$	0	0	$\sqrt{\delta - 2\xi_2 + \epsilon}$	$-\sqrt{\delta - 2\xi_2 - \epsilon}$	$-(\delta - 2\xi_2 - \epsilon)^2/2$
$r_8 =$	0	0	$-\sqrt{\delta - 2\xi_2 + \epsilon}$	$\sqrt{\delta - 2\xi_2 - \epsilon}$	$-(\delta - 2\xi_2 - \epsilon)^2/2$

3.2 Order of the GSQPTs

3.3 Critical points associated with ESQPTs

4. Results for two KPOs, $N_c = 2$

We start checking the dependence with the coupling constant of the first energy levels in the spectrum of two coupled non-identical and identical Kerr resonators. This is equivalent to the transition from local to normal states in coupled oscillators.

4.1 Non-identical Kerr oscillators

In this case we choose as system parameters

$$\delta_1 = \delta_2 = 0 \ , \quad \kappa = K_2/K_1 = \frac{\pi}{2} \ , \quad (\xi_{2,1}, \xi_{2,2}) = \{(0,0), (0.751, 0), (0.751, 2.533)\} \ . \quad (4.1)$$

In all cases the Fock basis $|n_1, n_2\rangle$ for both local Kerr oscillators has been truncated for a dimension $dim = 51$ and the coupling constant has been explored in the range $\xi_c \in [0, 3]$.

Results for the $\xi_2 = (0, 0)$ case are shown in Fig. 4.1. In the no coupling case the energies are analytic, and the eigenstates are $|n_1, n_2\rangle$ Fock states. In accordance with the labels in the figure

A $E_A = 0$. Four degenerate states: $|0,0\rangle, |0,1\rangle, |1,0\rangle, |1,1\rangle$.

B $E_B = 2$. Two degenerate states: $|2,0\rangle, |2,1\rangle$.

C $E_C = 2\kappa$. Two degenerate states: $|0,2\rangle, |1,2\rangle$.

D $E_D = 2 + 2\kappa$. Single state: $|2,2\rangle$.

E $E_E = 6$. Two degenerate states: $|3,0\rangle, |3,1\rangle$.

F $E_F = 6 + 2\kappa$. Single state: $|3,2\rangle$.

G $E_G = 6\kappa$. Two degenerate states: $|0,3\rangle, |1,3\rangle$.

H $E_H = 2 + 6\kappa$. Single state: $|2,3\rangle$.

States in Fig. 4.1 are depicted using dashed lines and the initial degeneracies for $\xi_c = 0$ are broken once the coupling constant is different from zero. The spectrum presents many level crossings that, in principle, should be avoided crossings.

We pay heed to the lower four energy levels, labeled as A in Fig. 4.1, and depict their correlation energy diagram, entanglement entropy, and participation ratio in Fig. 4.2.

Results for the $\xi_2 = (0.751, 0)$ case are shown in Fig. 4.3. In the zero ξ_c coupling case, energies are not analytic, as $\xi_{2,1} \neq 0$, but the eigenstate degeneracy can still be easily understood from the spectra of the individual oscillators. The first energies of the uncoupled Kerr with $\xi_{2,1} = 0.751$ are $\{-0.564001, -0.564001, 1.88572356, 5.75704623\}$. The states can then be labeled as $|n_1, n_2\rangle$, though in this case only the second oscillator eigenstates are pure Fock states. The first oscillator eigenstates are a mixture of Fock states. Taking this into consideration, the first states can be labeled in Fig. 4.3 as

A Four degenerate states: $|0,0\rangle, |0,1\rangle, |1,0\rangle, |1,1\rangle$.

B Two degenerate states: $|2,0\rangle, |2,1\rangle$.

C Two degenerate states: $|0,2\rangle, |1,2\rangle$.

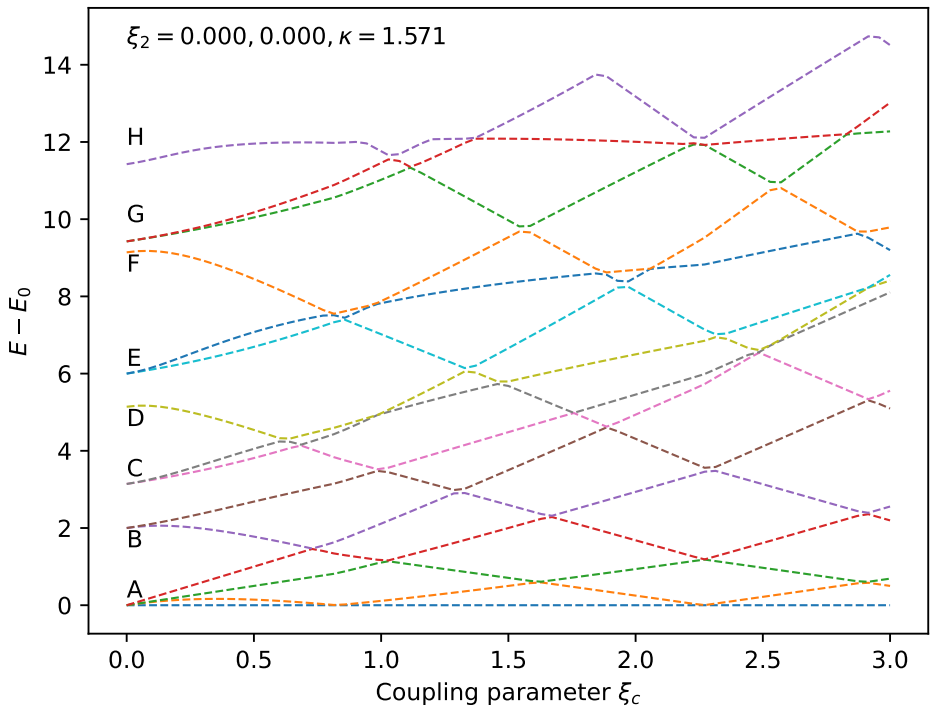

Figure 4.1: Correlation energy diagram for the first energy states of Hamiltonian (1.1) with control parameters $\delta_1 = \delta_2 = 0$, $\xi_{2,1} = \xi_{2,2} = 0$, and $\kappa = \pi/2$ for $\xi_c \in [0, 3]$. Calculations were carried out with a basis truncated and $n = 51$.

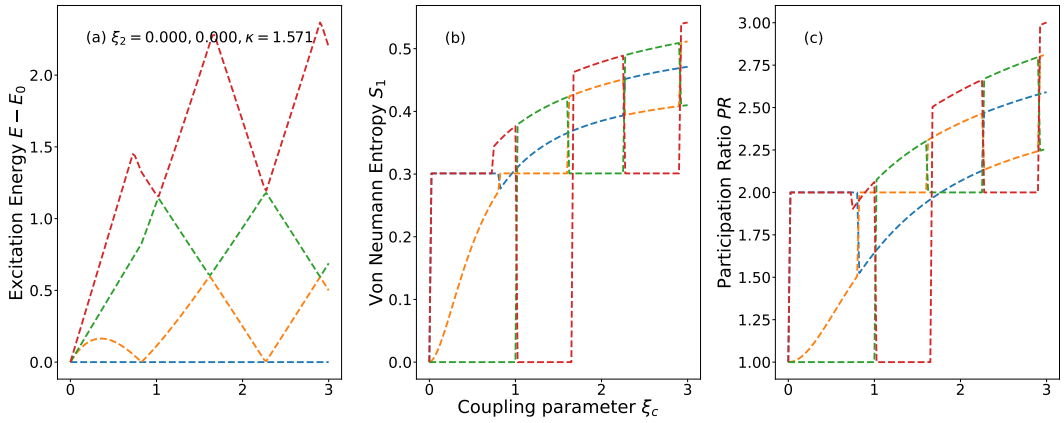

Figure 4.2: Correlation energy diagram (panel (a)), entanglement entropy (panel (b)), and participation ratio (panel (c)) for the first four energy states of Hamiltonian (1.1) with control parameters $\delta_1 = \delta_2 = 0$, $\xi_{2,1} = \xi_{2,2} = 0$, and $\kappa = \pi/2$ for $\xi_c \in [0, 3]$. Calculations were carried out with a basis truncated and $n = 55$.

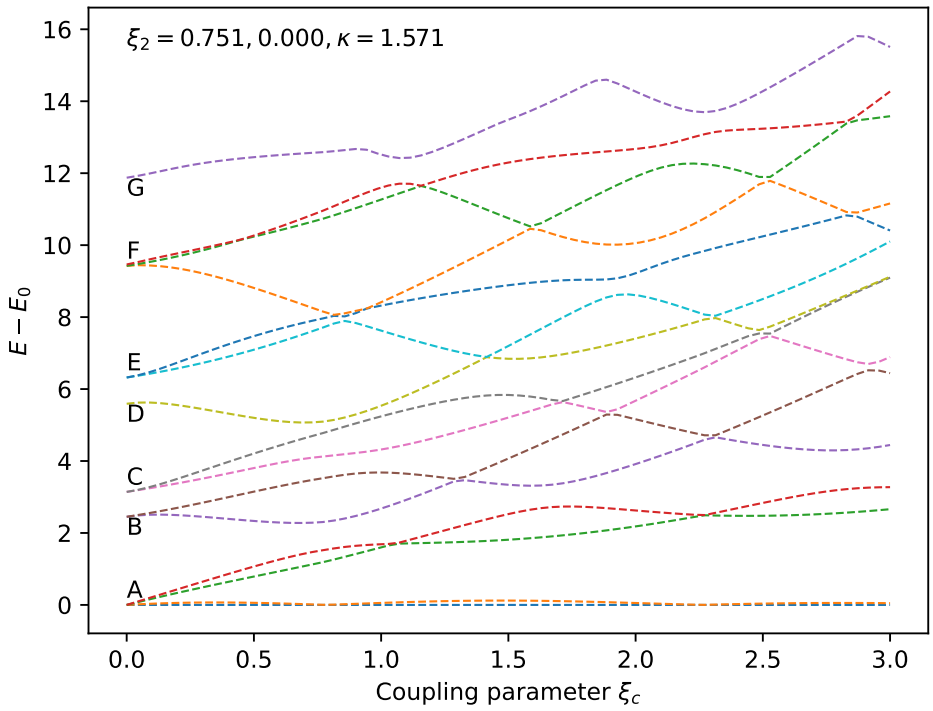

Figure 4.3: Correlation energy diagram for the first energy states of Hamiltonian (1.1) with control parameters $\delta_1 = \delta_2 = 0$, $\xi_{2,1} = 0.751, \xi_{2,2} = 0$, and $\kappa = \pi/2$ for $\xi_c \in [0, 3]$.. Calculations were carried out with a basis truncated and $n = 51$.

D Single state: $|2, 2\rangle$.

E Two degenerate states: $|3, 0\rangle, |3, 1\rangle$.

F Single state: $|3, 2\rangle$ plus two degenerate states: $|0, 3\rangle, |1, 3\rangle$. The three states are very close in energy.

G Single state: $|2, 3\rangle$.

As in the previous case, we depict in Fig. 4.4, results for the four lower states, labeled as A in Fig. 4.3.

Results for the third case considered, $\xi_2 = (0.751, 2.533)$, are shown in Fig. 4.5. In the zero coupling case, energies are not analytic, as $\xi_{2,1}$ and $\xi_{2.2}$ are different from zero. The eigenstate degeneracy can still be easily understood from the spectra of the individual oscillators. As in the previous case, the first energies of the uncoupled Kerr with $\xi_{2,1} = 0.751$ are $\{-0.564001, -0.564001, 1.88572356, 5.75704623\}$ and the energy of the $\xi_{2,2} = 2.533$ resonator are $\{-4.64861, -4.64861, 4.1583, 13.38963\}$. The states will be labeled again as $|n_1, n_2\rangle$, though in this case none of the single oscillator states are pure Fock states. Taking this into consideration, the first states can be labeled in Fig. 4.5 as

A Four degenerate states: $|0, 0\rangle, |0, 1\rangle, |1, 0\rangle, |1, 1\rangle$.

B Two degenerate states: $|2, 0\rangle, |2, 1\rangle$.

C Two degenerate states: $|3, 0\rangle, |3, 1\rangle$.

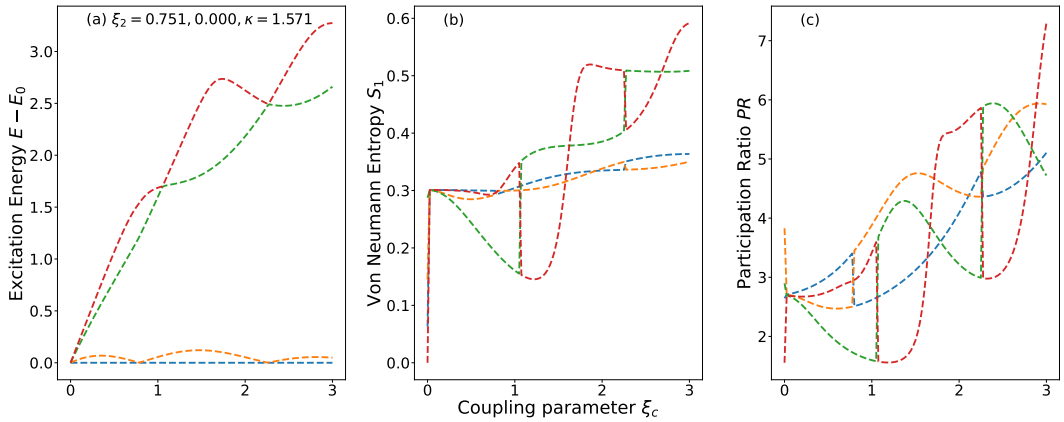

Figure 4.4: Correlation energy diagram (panel (a)), entanglement entropy (panel (b)), and participation ratio (panel (c)) for the first four energy states of Hamiltonian (1.1) with control parameters $\delta_1 = \delta_2 = 0$, $\xi_{2,1} = 0.751, \xi_{2,2} = 0$, and $\kappa = \pi/2$ for $\xi_c \in [0, 3]$. Calculations were carried out with a basis truncated and $n = 55$.

D Two degenerate states: $|0, 2\rangle, |1, 2\rangle$.

E Single state: $|2, 2\rangle$.

F Two degenerate states: $|0, 3\rangle, |1, 3\rangle$.

G Two degenerate states: $|4, 0\rangle$, $|4, 1\rangle$.

We again depict results for the lower four energy levels, labeled as A in Fig. 4.5, and depict their correlation energy diagram, entanglement entropy, and participation ratio in Fig. 4.6.

We also check the dependence of the correlation energy diagram for the excitation energy of the first energy levels as a function of the coupling parameter $\xi_c \in [0, 3]$ with different values of the detuning parameters, δ_1 and δ_2. We first calculate the correlation energy diagram as a function of the coupling parameter, ξ_c, for $\kappa = \pi/2$, $\xi_2 = 0$ and $\delta_1 = \{0, 0.55, 1, 2\}$ for $\delta_2 = \{0, \delta_1, 2\delta_1\}$. In all cases the dimension of the basis for each local KPO is $N_i = 41$, $i = 1, 2$, and results are shown in Fig. 4.7.

We finally compute, with a basis of $N_i = 41$ for $i = 1, 2$, a correlation energy diagram for the first excitation energies as a function of the detuning parameter $\delta_1 \in [0, 4.5]$ with $\delta_2 = 1.5\delta_1$ and $\kappa = \pi/2$, $\xi_{2,1} = \xi_{2,2} = 0$ (left column panels) and $\xi_{2,1} = \xi_{2,2} = 0.5$ (right column panels) for $\xi_c = \{0.0, 0.5, 1.0, 2.0\}$ (see legends). Results are depicted in Fig. 4.8.

4.2 Identical Kerr oscillators

In this case it is possible to use a symmetry adapted basis and distinguish between even and odd parity states. We perform calculations for parameters equal to

$$\delta = 0 \ , \quad \xi_2 = \{0, 0.751\} \ . \tag{4.2}$$

As in the previous case, the Fock basis $|n_1, n_2\rangle$ for both local Kerr oscillators has been truncated for a dimension $dim = 51$ and the coupling constant has been explored in the range $\xi_c \in [0, 3]$.

Results for $\xi_2 = 0$ and even states is shown with bright orange lines in Fig. 4.9 where the first states have been labeled as

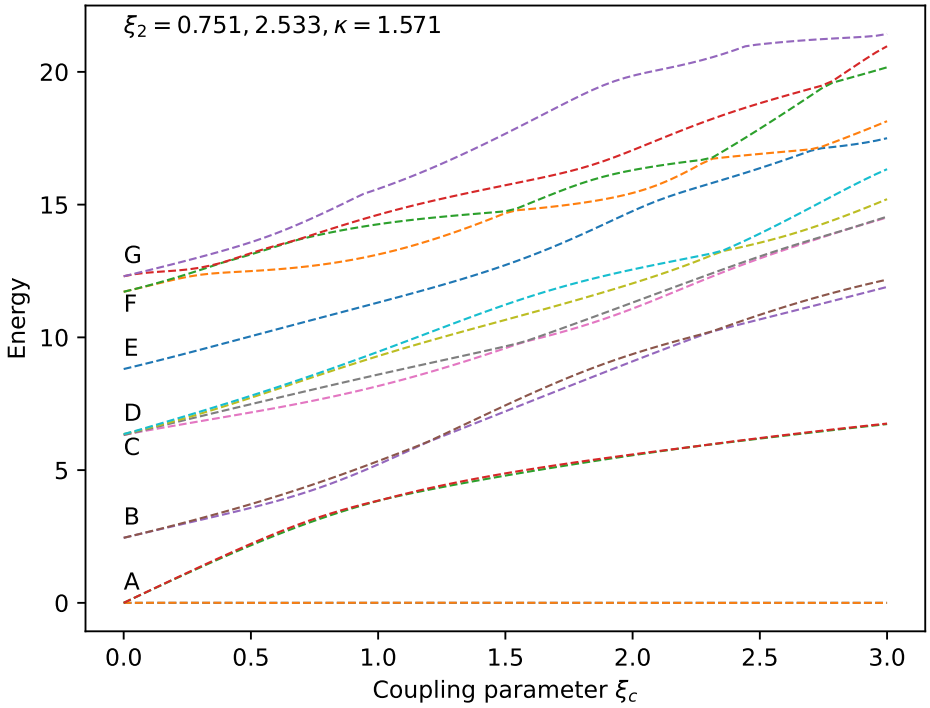

Figure 4.5: Correlation energy diagram for the first energy states of Hamiltonian (1.1) with control parameters $\delta_1 = \delta_2 = 0$, $\xi_{2,1} = 0.751, \xi_{2,2} = 2.533$, and $\kappa = \pi/2$ for $\xi_c \in [0, 3]$.

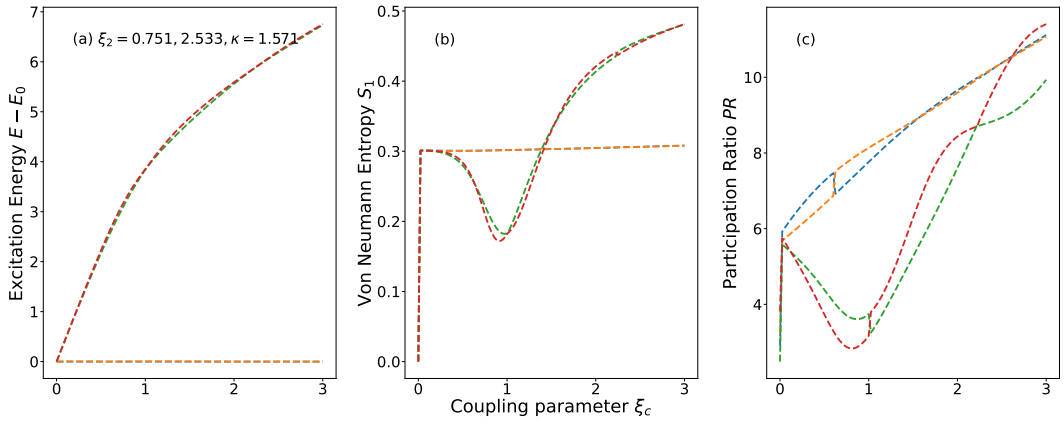

Figure 4.6: Correlation energy diagram (panel (a)), entanglement entropy (panel (b)), and participation ratio (panel (c)) for the first four energy states of Hamiltonian (1.1) with control parameters $\delta_1 = \delta_2 = 0$, $\xi_{2,1} = 0.751, \xi_{2,2} = 2.533$, and $\kappa = \pi/2$ for $\xi_c \in [0, 3]$. Calculations were carried out with a basis truncated and $n = 55$.

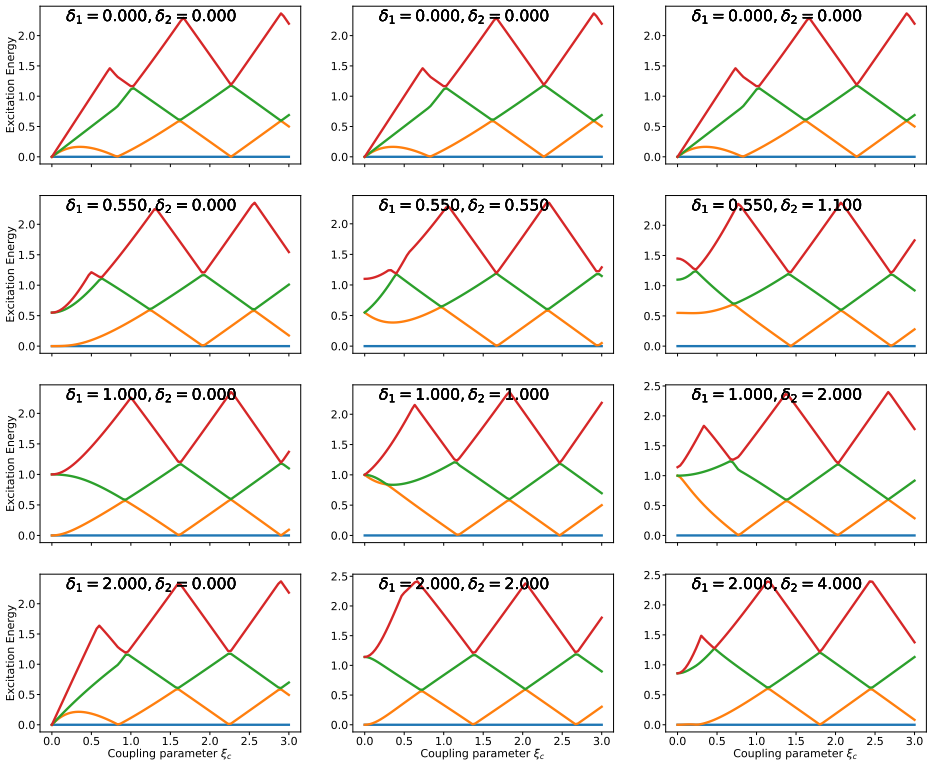

Figure 4.7: Correlation energy diagram for the first energy states of Hamiltonian (1.1) as a function of ξ_c with control parameters $\kappa = \pi/2$, $\xi_{2,1} = \xi_{2,2} = 0$, $\kappa = \pi/2$, and $\delta_1 = \{0, 0.55, 1, 2\}$ for $\delta_2 = \{0, \delta_1, 2\delta_1\}$ (one value per column, see legends). The coupling parameter is varied in the range $\xi_c \in [0, 3]$. All calculations are carried out with $N_i = 41$ for $i = 1, 2$.

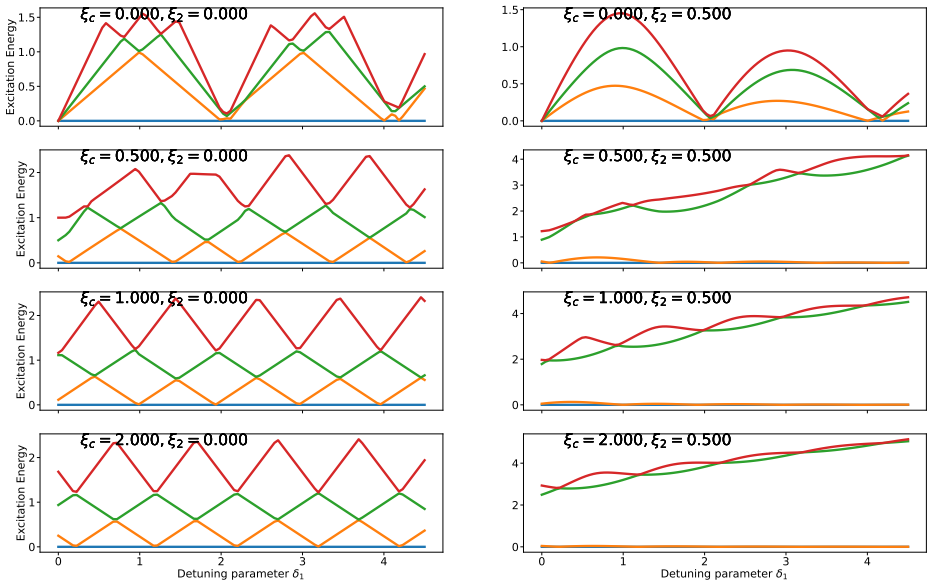

Figure 4.8: Correlation energy diagram for the first energy states of Hamiltonian (1.1) as a function of δ_1 with control parameters $\xi_{2,1} = \xi_{2,2} = 0$ and 0.5, $\kappa = \pi/2$, and $\xi_c = \{0, 0.5, 1, 2\}$ (one value per column, see legends). The coupling parameter is varied in the range $\delta_1 \in [0, 4.5]$ and $\delta_2 = 1.5\delta_1$. All calculations are carried out with $N_i = 41$ for $i = 1, 2$.

A Three degenerate states: $|0,0\rangle, |0,1\rangle^+, |1,1\rangle$.

B Two degenerate states: $|2,0\rangle^+, |2,1\rangle^+$.

C Single state: $|2,2\rangle$.

D Two degenerate states: $|3,0\rangle^+, |3,1\rangle^+$.

E Single state: $|3,2\rangle^+$.

We have introduced the notation $|n_1, n_2\rangle^\pm$ for $n_1 \neq n_2$

$$|n_1, n_2\rangle^\pm = \frac{1}{\sqrt{2}} \left(|n_1, n_2\rangle \pm |n_2, n_1\rangle \right) \ . \tag{4.3}$$

We are interested in the lower energy states and we have depicted the energy, Von Neumann entropy, and participation ratio in the local basis as a function of ξ_c for the first four even eigenstates (states A and lower energy state B in Fig. 4.9) in Fig. 4.10.

In the odd case, the corresponding first odd states are shown in Fig. 4.11 and labeled as

A Single state: $|0,1\rangle^-$.

B Two degenerate states: $|2,0\rangle^-, |2,1\rangle^-$.

C Two degenerate states: $|3,0\rangle^-, |3,1\rangle^-$.

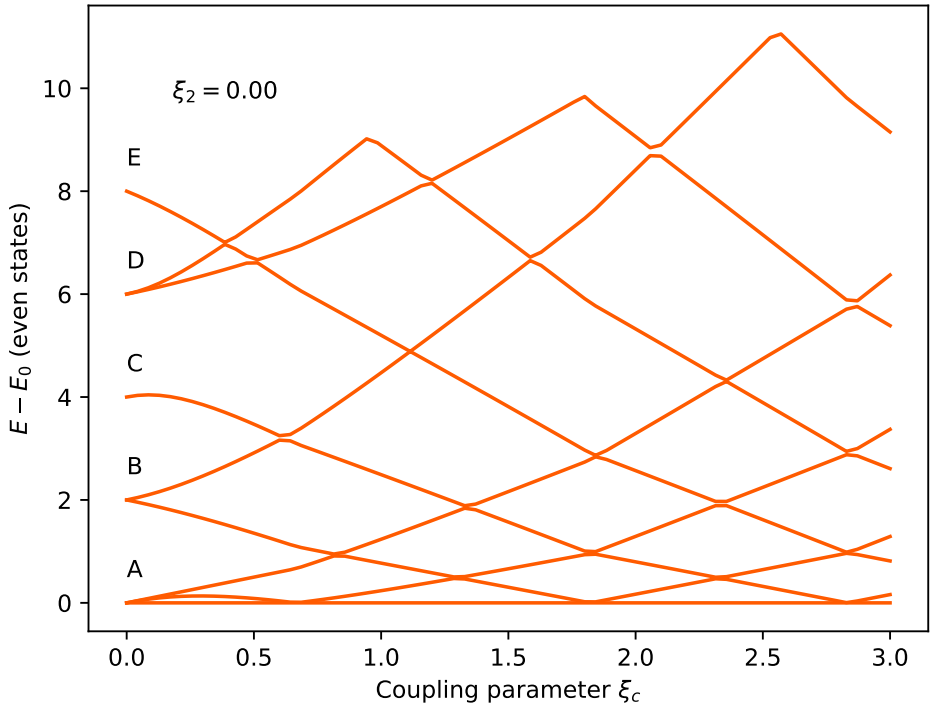

Figure 4.9: Correlation energy diagram for the first even parity energy states of Hamiltonian (1.2) with control parameters $\delta = 0$ and $\xi_2 = 0.0$ for $\xi_c \in [0, 3]$. Calculations were carried out using a coupled basis with $N_i = 51$ for $i = 1, 2$.

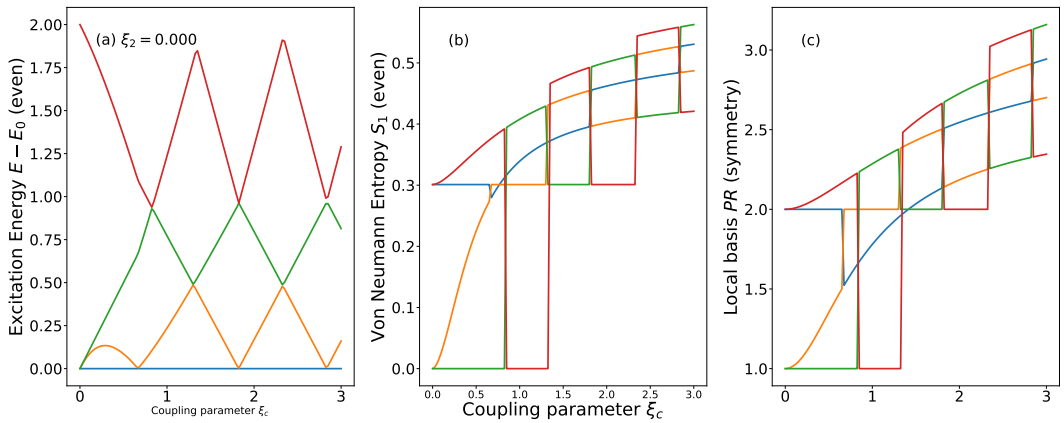

Figure 4.10: Correlation energy diagram for the lowest energy even parity states of Hamiltonian (1.2) with control parameters $\delta = 0$ and $\xi_2 = 0.0$ for $\xi_c \in [0, 3]$. Calculations were carried out using a coupled basis with $N_i = 51$ for $i = 1, 2$.

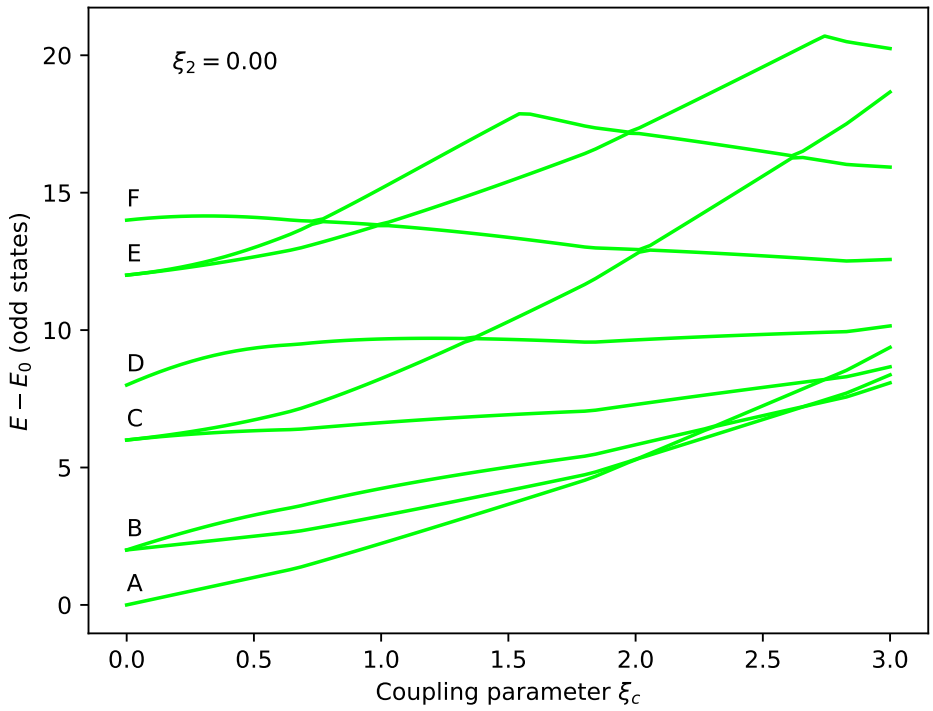

Figure 4.11: Correlation energy diagram for the first odd parity energy states of Hamiltonian (1.2) with control parameters $\delta = 0$ and $\xi_2 = 0.0$ for $\xi_c \in [0, 3]$. Calculations were carried out using a coupled basis with $N_i = 51$ for $i = 1, 2$.

D Single state: $|3, 2\rangle^-$.

E Two degenerate states: $|4, 0\rangle^-, |4, 1\rangle^-$.

F Single state: $|4, 2\rangle^-$.

As in the even case, we have depicted the energy, Von Neumann entropy, and participation ratio in the local basis as a function of ξ_c for the first four even eigenstates (states A, B, and lower energy state C in Fig. 4.11) in Fig. 4.12.

We have also depicted the correlation energy diagram for the first even and odd state with a non-zero value of the squeezing parameter, $\xi_2 = 0.751$, in Figs. 4.13 and 4.15. Calculations were carried out using a coupled basis with $N_i = 51$ for $i = 1, 2$. The energy, von Neumann entropy, and participation ratio for the first four energy levels in this case can be found in Figs. 4.14 and 4.16.

We can in this case also explore the effect of the detuning parameter, δ, in the Hamiltonian Eq. (1.3). To do so we first plot the correlation energy diagram for the first even(odd) states depicted using full(dashed) lines in Fig. 4.17 as a function of the coupling control parameter ξ_c for $\xi_2 = \{\}$ and $\delta = \{\}$. We also plot a correlation energy diagram as a function of the detuning parameter, δ, for fixed values of the coupling control parameter $\xi_c = \{\}$ and of $\xi_2 = \{\}$. In the second case, we again distinguish between even and odd states, depicting them using full lines in Fig. 4.19 and dashed lines in Fig. 4.20, respectively.

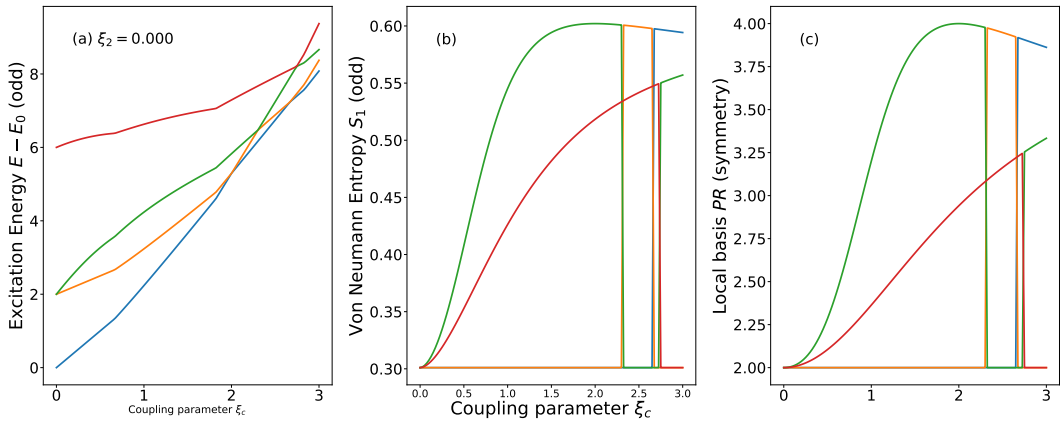

Figure 4.12: Correlation energy diagram for the lowest energy odd parity states of Hamiltonian (1.2) with control parameters $\delta = 0$ and $\xi_2 = 0.0$ for $\xi_c \in [0, 3]$.
Calculations were carried out using a coupled basis with $N_i = 51$ for $i = 1, 2$.

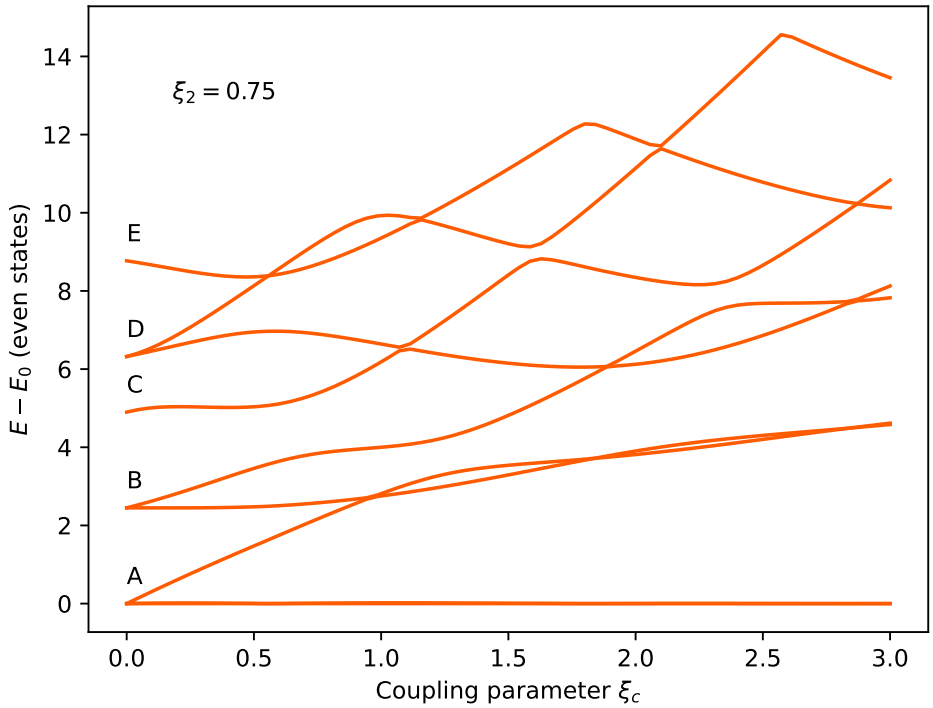

Figure 4.13: Correlation energy diagram for the first even parity energy states of Hamiltonian (1.2) with control parameters $\delta = 0$ and $\xi_2 = 0.751$ for $\xi_c \in [0, 3]$. Calculations were carried out using a coupled basis with $N_i = 51$ for $i = 1, 2$.

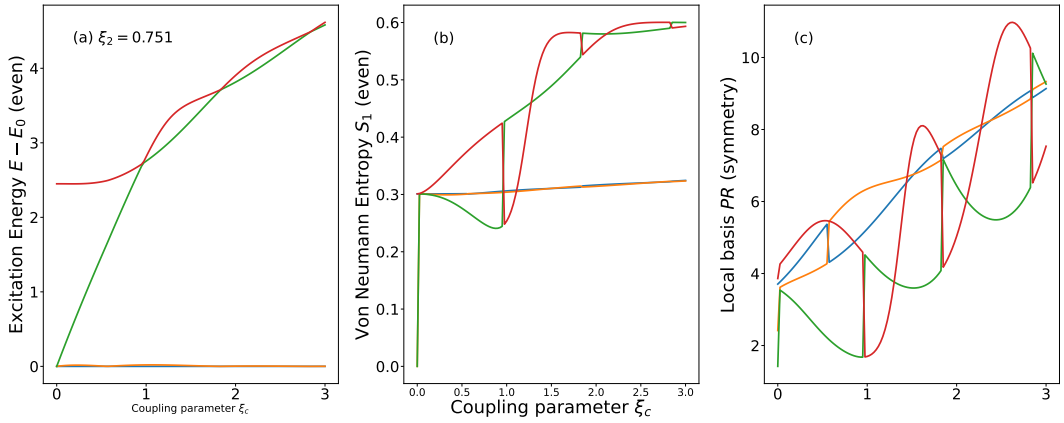

Figure 4.14: Panel (a): Correlation energy diagram. Panel (b) Von Neumann entropy. Panel (c) Participation Ratio (local basis). All panels: results for the lowest four energy odd parity states of Hamiltonian (1.2) with control parameters $\delta = 0$ and $\xi_2 = 0.751$ for $\xi_c \in [0, 3]$.
Calculations were carried out using a coupled basis with $N_i = 51$ for $i = 1, 2$.

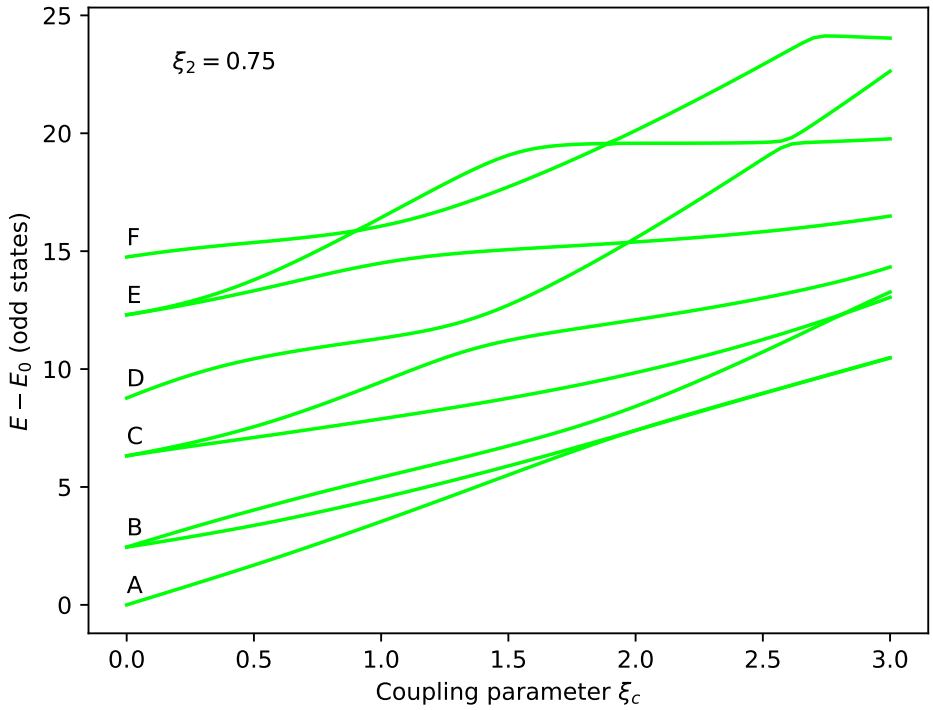

Figure 4.15: Correlation energy diagram for the first odd parity energy states of Hamiltonian Eq. (1.2) with control parameters $\delta = 0$ and $\xi_2 = 0.751$ for $\xi_c \in [0, 3]$. Calculations were carried out using a coupled basis with $N_i = 51$ for $i = 1, 2$.

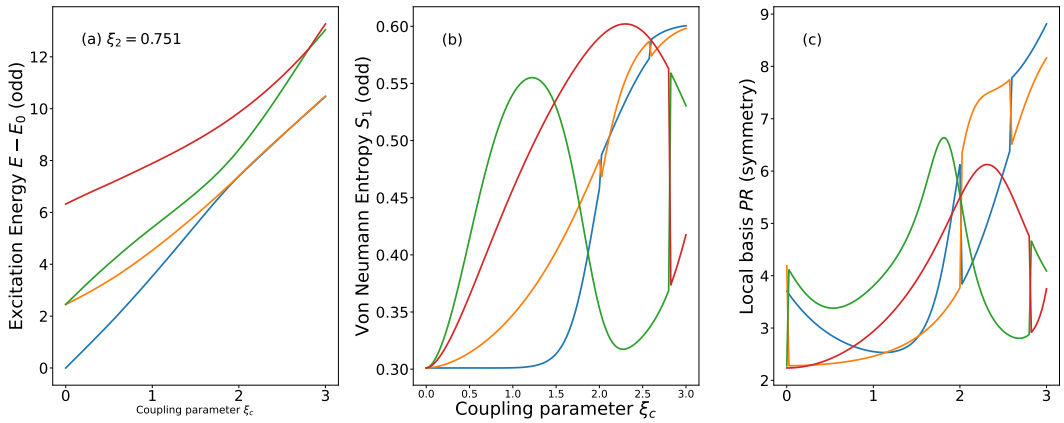

Figure 4.16: Panel (a): Correlation energy diagram. Panel (b) Von Neumann entropy. Panel (c) Participation Ratio (local basis). All panels: results for the lowest four energy odd parity states of Hamiltonian (1.2) with control parameters $\delta = 0$ and $\xi_2 = 0.751$ for $\xi_c \in [0, 3]$. Calculations were carried out using a coupled basis with $N_i = 51$ for $i = 1, 2$.

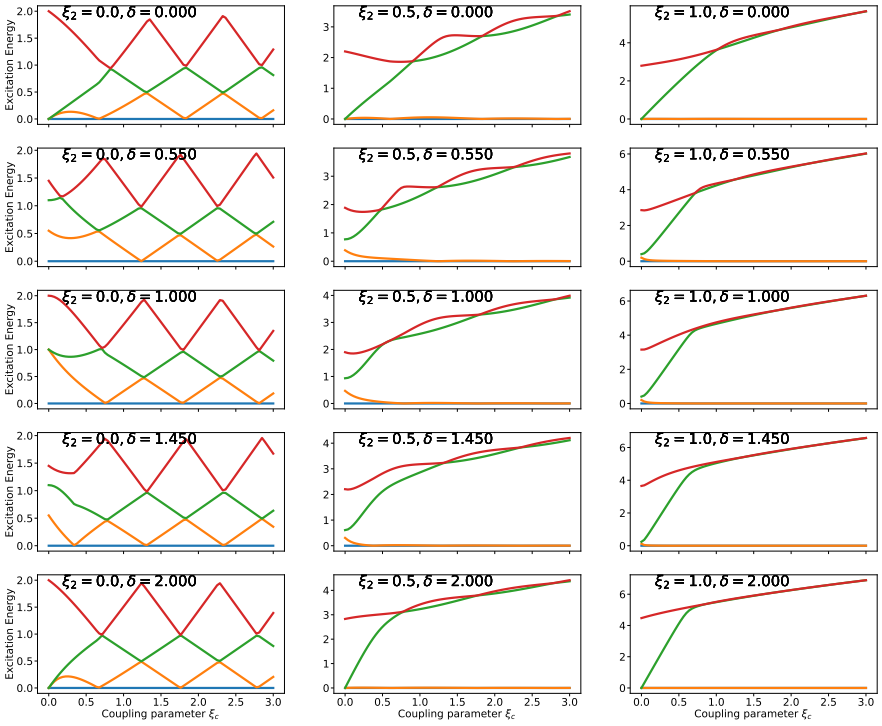

Figure 4.17: Correlation energy diagram for the first even excitation levels of the identical coupled Kerr resonators Hamiltonian Eq. (1.3) as a function of the coupling parameter ξ_c for detuning parameter values $\delta = \{0, 0.55, 1, 1.45, 2\}$ and two-photon squeezing $\xi_2 = \{0, 0.5, 1.0\}$. Calculations were carried out using a coupled basis with $N_i = 51$ for $i = 1, 2$.

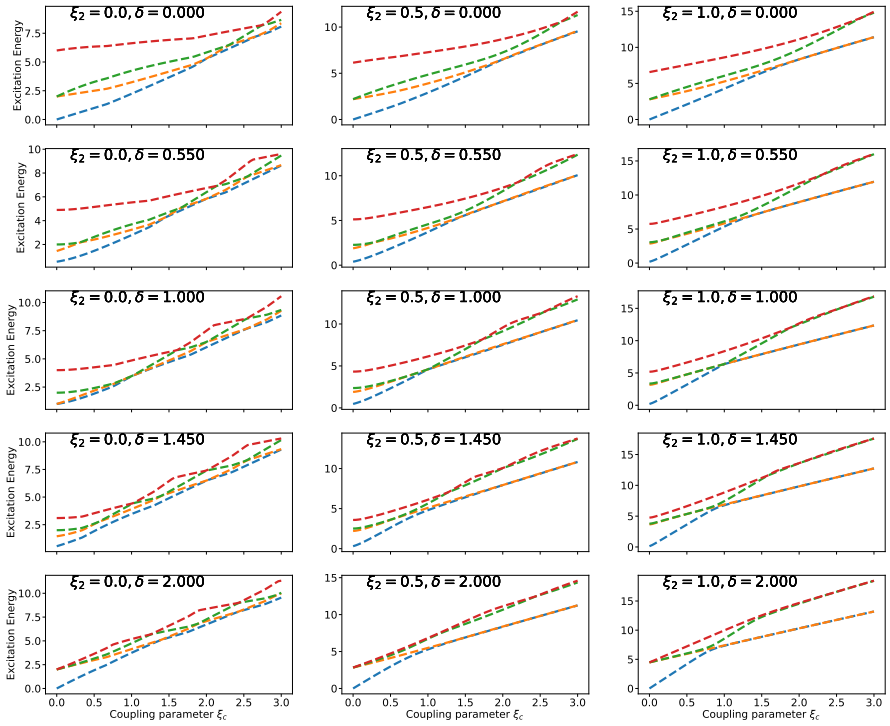

Figure 4.18: Correlation energy diagram for the first odd excitation levels of the identical coupled Kerr resonators Hamiltonian Eq. (1.3) as a function of the coupling parameter ξ_c for detuning parameter values $\delta = \{0, 0.55, 1, 1.45, 2\}$ and two-photon squeezing $\xi_2 = \{0, 0.5, 1.0\}$. Calculations were carried out using a coupled basis with $N_i = 51$ for $i = 1, 2$.

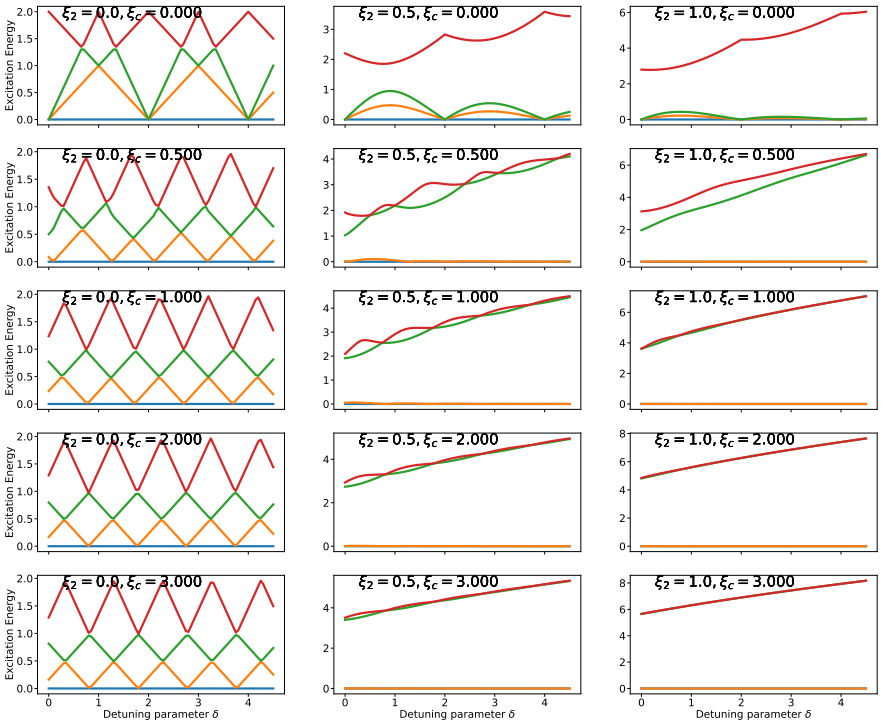

Figure 4.19: Correlation energy diagram for the first even excitation levels of the identical coupled Kerr resonators Hamiltonian Eq. (1.3) as a function of the detuning parameter δ for coupling parameter values $\xi_c = \{0, 0.5, 1, 2, 3\}$ and two-photon squeezing $\xi_2 = \{0, 0.5, 1.0\}$. Calculations were carried out using a coupled basis with $N_i = 51$ for $i = 1, 2$.

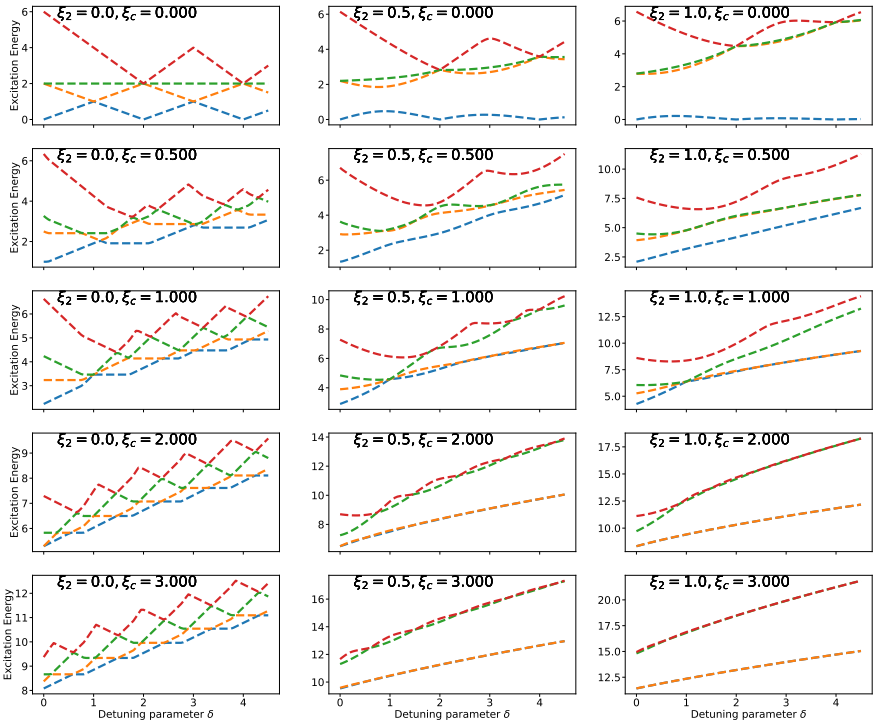

Figure 4.20: Correlation energy diagram for the first odd excitation levels of the identical coupled Kerr resonators Hamiltonian Eq. (1.3) as a function of the detuning parameter δ for coupling parameter values $\xi_c = \{0, 0.5, 1, 2, 3\}$ and two-photon squeezing $\xi_2 = \{0, 0.5, 1.0\}$. Calculations were carried out using a coupled basis with $N_i = 51$ for $i = 1, 2$.

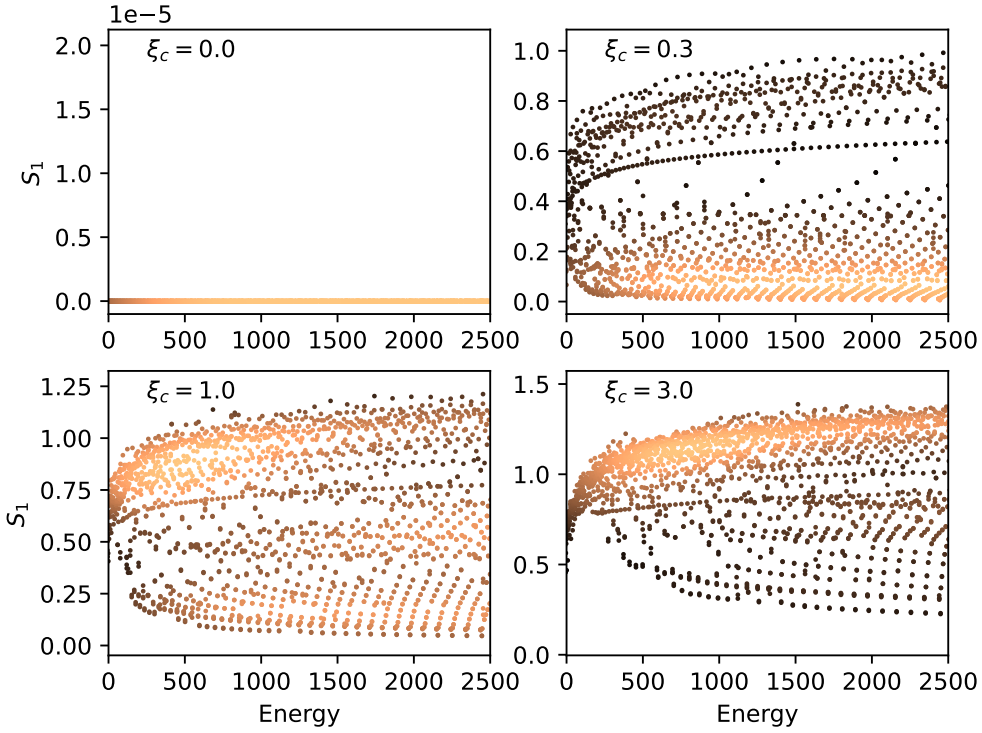

Figure 4.21: Von Neumann entropy for eigenstates of Hamiltonian (1.1) using Ref. [4] parameters in Eq. (4.4) and $\xi_c = \{0, 0.3, 1, 3\}$. The calculation has been truncated at $N_1 = N_2 = 70$.

4.3 Chaos in Coupled Kerr Resonators

We start with a system of two non-identical Kerr resonators as the ones defined by Goto in Ref. [4] with parameters

$$\begin{aligned} \delta_1 = 0 \ , \quad \delta_2 = 0 \\ \xi_{2,1} = 3 \ , \quad \xi_{2,2} = \pi \\ \kappa = 1.0 \ , \quad \kappa = \frac{K_2}{K_1} \end{aligned} \tag{4.4}$$

We consider that $J_{12} = J_{21} = 1$ and the three ξ_c values selected by Goto plus a fourth one: $\xi_c = \{0, 0.3, 1, 3\}$. The calculations are carried out in a notebook[1] where we truncate the one-body KPO basis at a dimension of the Fock space $dim = 80$ for each resonator. We have plotted the Peres lattices for the Von Neumann entropy (or entanglement entropy) for subsystem 1 in Fig. 4.21, the participation ratio in Fig. 4.22, the expectation value of $\hat{n}_i$ with $i = 1, 2$ in Figs. 4.23 and 4.24, and the density of states in Fig. 4.25.

Expectation value of $\hat{n}_i$:

Density of states:

[1] `coupled_Kerr_Nc_2_CED_symm_calc-GOTO.ipynb` in GitLab project `coupled_KPOs`.

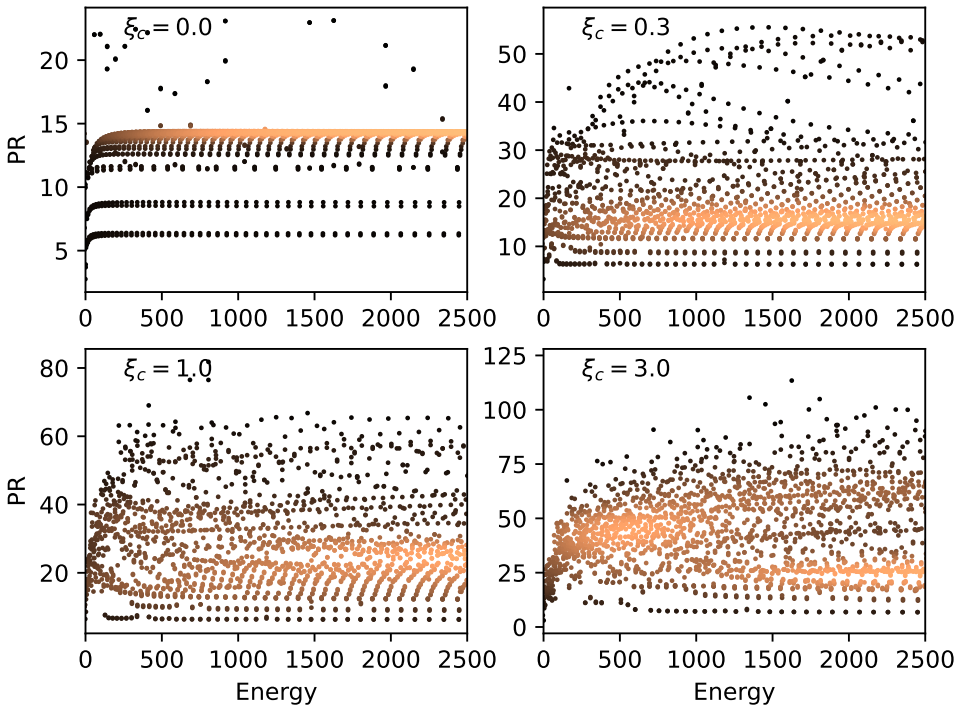

Figure 4.22: Participation ratio of eigenstates of Hamiltonian (1.1) using Ref. [4] parameters (4.4) and $\xi_c = \{0, 0.3, 1, 3\}$. The calculation has been truncated at $N_1 = N_2 = 80$.

Bibliography

[1] Hayato Goto. Quantum computation based on quantum adiabatic bifurcations of kerr-nonlinear parametric oscillators. *Journal of the Physical Society of Japan*, 88(6):061015, 2019.
Compare KPOs with Optical Parametric Oscillators (OPOs). Excellent Table I with formulas for both cases. Some results for $N_c = 2$. Interesting discussion of the KPO system as an Quantum bifurcation machine and its relation with the Ising problem solution.

[2] Hayato Goto. Bifurcation-based adiabatic quantum computation with a nonlinear oscillator network. *Scientific Reports*, 6(1):21686, 2016.
Precedes [1] and it is very related to it.

[3] Pavel Cejnar, Pavel Stránský, Michal Macek, and Michal Kloc. Excited-state quantum phase transitions. *Journal of Physics A: Mathematical and Theoretical*, 54(13):133001, mar 2021.
ESQPT review article.

[4] Hayato Goto and Taro Kanao. Chaos in coupled kerr-nonlinear parametric oscillators. *Phys. Rev. Res.*, 3:043196, Dec 2021.
Chaos in coupled Kerr oscillators. Classical alculations: Poincaré sections, an alternative to Poincaré sections, and sensitivity to initial conditions. Quantum calculations: level statistics, OTOC, and Husimi/Wigner time dependence of initial $|0\rangle$ state.

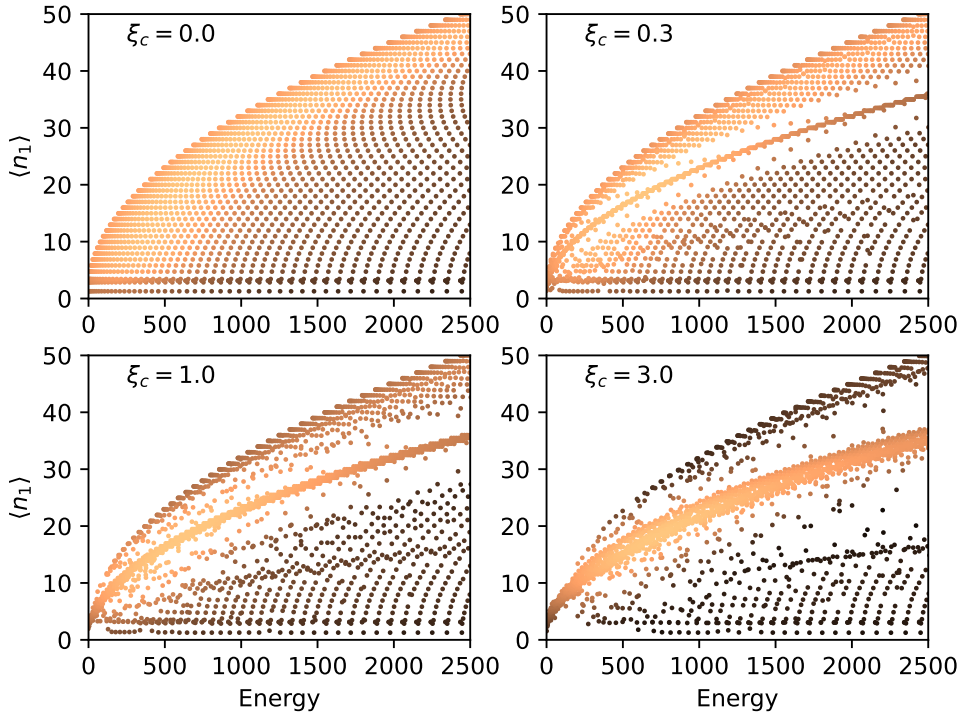

Figure 4.23: Expectation value of $\hat{n}_1$ for eigenstates of Hamiltonian (1.1) using Ref. [4] parameters (4.4) and $\xi_c = \{0, 0.3, 1, 3\}$. The calculation has been truncated at $N_1 = N_2 = 80$.

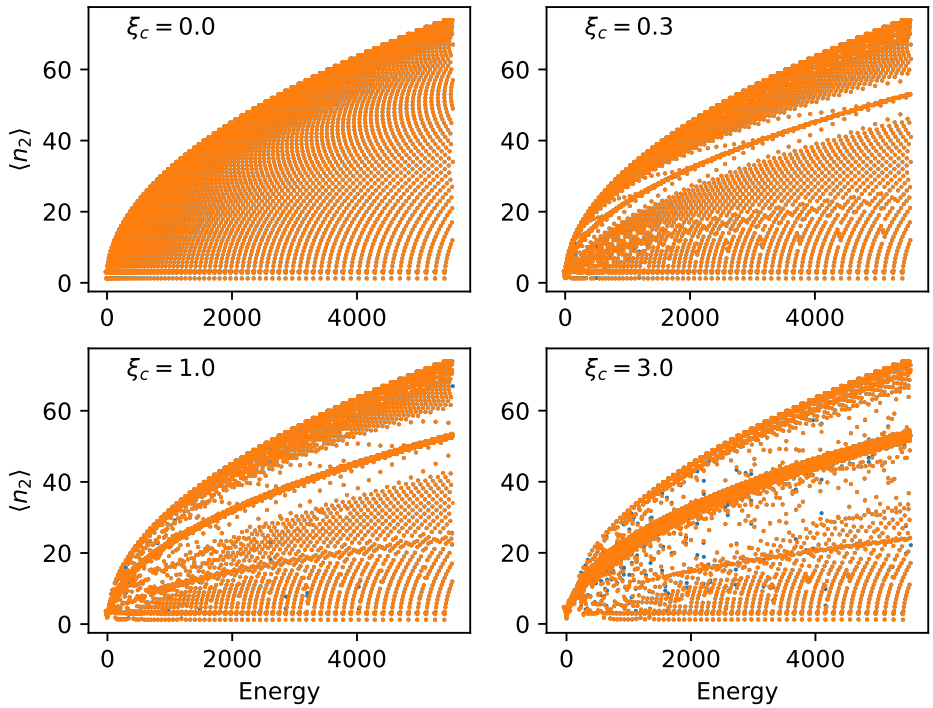

Figure 4.24: Expectation value of $\hat{n}_2$ for eigenstates of Hamiltonian (1.1) using Ref. [4] parameters (4.4) and $\xi_c = \{0, 0.3, 1, 3\}$. The calculation has been truncated at $N_1 = N_2 = 80$.

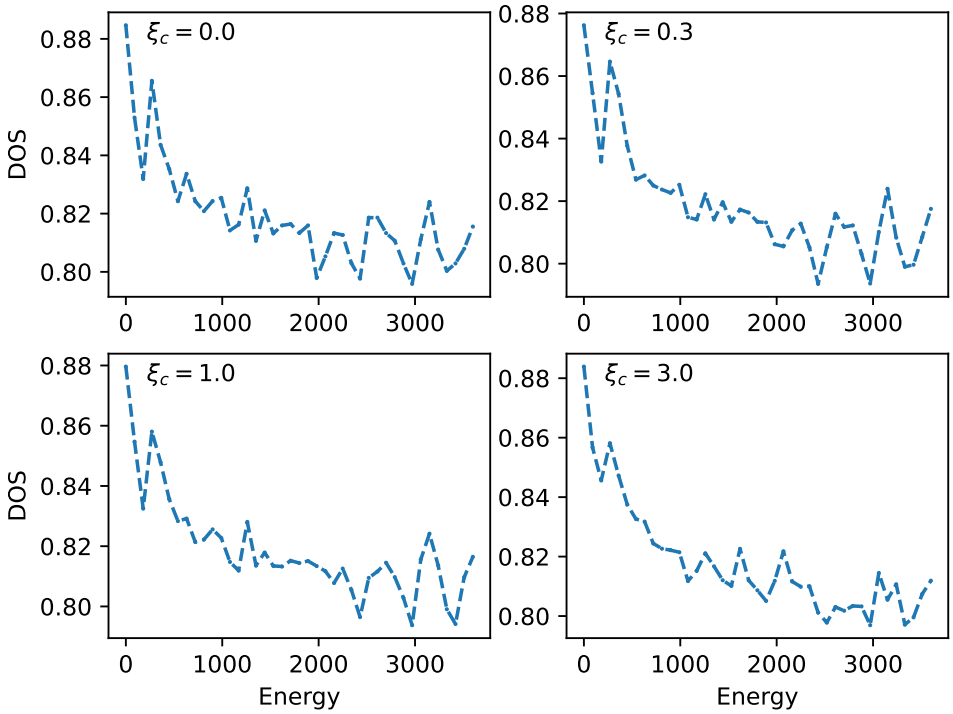

Figure 4.25: Density of states for eigenvalues of Hamiltonian (1.1) using Ref. [4] parameters (4.4) and $\xi_c = \{0, 0.3, 1, 3\}$. The calculation has been truncated at $N_1 = N_2 = 80$.